Kinetics of Folding of Guanidine-Denatured Hen Egg White Lysozyme and Carboxymethyl(Cys^{6},Cys^{127})-Lysozyme: A Stopped-Flow Absorbance and Fluorescence Study†

Mary E. Denton,‡ David M. Rothwarf, and Harold A. Scheraga*

Baker Laboratory of Chemistry, Cornell University, Ithaca, New York 14853-1301

Received April 7, 1994; Revised Manuscript Received July 11, 1994®

ABSTRACT: The folding kinetics of hen egg white lysozyme and of a three-disulfide derivative of lysozyme [carboxymethyl(Cys^{6},Cys^{127})-hen egg white lysozyme] have been studied by absorbance- and fluorescence-detected stopped-flow techniques. A "very-fast" phase with a time constant in the millisecond range has been observed by both absorbance and fluorescence when unfolded lysozyme in 4 M guanidine hydrochloride, 100 mM phosphate buffer, and pH 2.0 is refolded at 0.5 M guanidine hydrochloride, 100 mM phosphate, and pH 6.7. Data obtained from fluorescence-detected refolding studies show that a transient intermediate is formed during the very-fast refolding phase. This intermediate is characterized by substantial quenching of tryptophan fluorescence. In addition, analysis of the fluorescence data indicates the presence of an additional "burst" phase that occurs within the dead time of the instrument, <3 ms. The very-fast phase is not observed during the refolding of the three-disulfide derivative. In addition, the three-disulfide derivative re-attains the final native folded conformation more rapidly than the unmodified protein over the range of temperatures studied (10–20 °C). We conclude that, not only does the presence of the disulfide bond between Cys^{6} and Cys^{127} slow down the overall folding process of lysozyme, but it also directs the folding of lysozyme through a pathway characterized by a non-native tertiary interaction(s).

While it is well-established that the amino acid sequence of a protein dictates its folded three-dimensional structure (Anfinsen, 1973), the mechanism by which proteins refold from their denatured state is not yet known. An understanding of how proteins fold requires a detailed determination of the intermediates and transition states that occur along the folding pathway. Toward this end, considerable effort has focused on the determination and characterization of intermediates populated during the folding process. Unfortunately, the identification of intermediates is hampered by the highly cooperative nature of the folding process. Furthermore, the determination of folding pathways and transition state structures is based on the assumption that structural intermediates observed during folding are the kinetically important intermediates, an assumption that is often difficult to prove. A wide variety of experimental techniques have been used to try to surmount these difficulties and elucidate the mechanism of protein folding (Kim & Baldwin, 1990; Matthews, 1993) including mutational studies (Jennings et al., 1991; Shortle, 1992), disulfide-bond trapping studies (Scheraga et al., 1984; Creighton, 1986; Weissman & Kim, 1991; Rothwarf & Scheraga, 1993a,b), hydrogen-exchange studies (Englander & Mayne, 1992; Baldwin, 1993), studies of thermodynamically stable partially-folded species (Kuwajima, 1989; Haynie & Friere, 1993), and studies of peptide models (Oas & Kim, 1988; Montelione & Scheraga, 1989; Dyson & Wright, 1993). However, despite this considerable effort, no clear unifying principles have yet emerged. Here, we present a detailed study of the refolding of guanidine-denatured hen egg white lysozyme and a three-disulfide derivative carried out by absorbance- and fluorescence-detected stopped-flow techniques. These studies shed new light on the nature of the intermediate and transition states of protein folding.

Hen egg white lysozyme, a well-characterized protein whose X-ray crystal structure (Blake et al., 1965; Strynadka & James, 1991) and NMR solution structure (Smith et al., 1993) are known, has been studied extensively in kinetic folding experiments [for a review see Dobson et al. (1994)]. In early renaturation studies carried out by measuring the stopped-flow absorbance kinetics of lysozyme, Kato et al. (1981) demonstrated that two kinetic phases were observed when the protein was jumped from 4 M GdnHCl,[1] pH 2.5, to 0.5 M GdnHCl, pH 2.6, and 25 °C. These were designated as the fast and slow phases with time constants (τ) of approximately 1 and 17 s, respectively. In addition, evidence for a third phase, $\tau \leq 20$ ms, buried in the mixing time, was inferred from the difference between the sum of the absorbance amplitudes observed in the kinetic refolding experiments and the absorbance difference between the equilibrium unfolded and native protein.

By using near- and far-UV CD to follow the refolding of lysozyme upon dilution from high to low concentrations of GdnHCl, Kuwajima et al. (1985) demonstrated the presence of a transient folding intermediate that had a significantly ordered peptide backbone structure, but that had aromatic side chains in a conformation(s) indistinguishable from that of the unfolded protein. Likewise, in an NMR experiment in which the refolding process competed with amide hydrogen exchange, Miranker et al. (1991) identified an intermediate of lysozyme in which the amide protons of one of its two subdomains showed significant protection against exchange.

More recent studies of lysozyme refolding from the guanidine-denatured form, using pulsed hydrogen/deuterium

† This work was supported by Grant GM-14312 from the National Institute of General Medical Sciences of the National Institutes of Health.

* Author to whom correspondence should be addressed.

‡ Present address: ImmunoGen, Inc., 333 Providence Highway, Norwood, MA 02062.

® Abstract published in *Advance ACS Abstracts,* September 1, 1994.

[1] Abbreviations: 3SS-lysozyme, carboxymethyl(Cys^{6},Cys^{127})-lysozyme; GdnHCl, guanidine hydrochloride.

0006-2960/94/0433-11225$04.50/0

exchange (H/D exchange) (Radford et al., 1992) and stopped-flow CD (Radford et al., 1992; Chaffotte et al., 1992), have presented additional information about the folding process. On the basis of these methods, Radford et al. (1992) suggested that the folding pathway of lysozyme at pH 5.5 involves rapid formation of labile α-helical structure within the first 2 ms followed by protection of $\sim$50% of the α-helical amides and $\sim$30% of the β-structure within the next 10–20 ms. Most of the α-helical structure is completely folded by 100–150 ms, while the folding of the β-structure-containing portion (β-domain) of the protein is not complete until $\sim$1 s. On the basis of these results, Radford et al. (1992) proposed that multiple refolding pathways are populated during the refolding process. On the basis of stopped-flow and continuous-flow CD measurements, Chaffotte et al. (1992) concluded that, at pH 7.8, 100% of the secondary structure has formed within the burst phase (the first 4 ms) and that the correct tertiary contacts are completely formed within the next second. Both CD studies have detected an unusual phase in the far-UV CD (at 222 and 225 nm) in which the observed amount of secondary structure is 150–175% that of the native protein, with the minimum in the CD signal occurring at 80–100 ms into the refolding. Radford et al. (1992) suggested that this phase probably corresponds to some non-native interaction. Chaffotte et al. (1992) suggested that this phase originates from a transient constraint on a disulfide bond.

A related objective in the elucidation of the folding process has been to determine the role of disulfide bonds during folding. Previously, Denton and Scheraga (1991) and Radford et al. (1991) have reported the preparation and characterization of a three-disulfide form of lysozyme [carboxymethyl(Cys^6,-Cys^{127})-hen egg white lysozyme, hereafter referred to as 3SS-lysozyme] in which the disulfide bond between Cys^6 and Cys^{127} was selectively reduced and each resulting half-cystine irreversibly modified by iodoacetate. The conformation of 3SS-lysozyme was demonstrated to be predominantly native-like with a local perturbation of structure around the site of modification (Denton & Scheraga, 1991; Radford et al., 1991). A recent crystal structure of 3SS-lysozyme confirmed that its structure is very similar to that of unmodified lysozyme except for some displacement of the C-terminal residues (Hill et al., 1993). Although 3SS-lysozyme exhibits approximately 85% of the activity of unmodified lysozyme, removal of this disulfide bond from lysozyme greatly reduces the stability of the protein because of chain entropy effects (Denton & Scheraga, 1991; Cooper et al., 1992).

By carrying out stopped-flow absorbance and fluorescence kinetic measurements on both lysozyme and 3SS-lysozyme, it has been possible to gain new insights into the folding process-(es) of lysozyme. The results presented here demonstrate that, not only does the presence of the disulfide bond between Cys^6 and Cys^{127} slow down the folding process, but it also constrains lysozyme to fold through a pathway which is characterized by a non-native tertiary interaction involving a tryptophan residue(s). We will reinterpret the results of previous kinetic studies in light of the data presented here and provide possible folding mechanisms consistent with all of the published data.

MATERIALS AND METHODS

Materials. Hen egg white lysozyme (Sigma Chemical Co., grade I) and 3SS-lysozyme were prepared and purified according to previously reported procedures (Denton & Scheraga, 1991). GdnHCl, ultrapure grade, was obtained from ICN Biochemicals, Inc. Phosphate buffers were prepared using HPLC-grade phosphoric acid (Fisher Scientific Co.).

Circular Dichroism Spectroscopy. Circular dichroism spectra of 3SS-lysozyme and unmodified lysozyme under the final refolding conditions (0.5 M GdnHCl, 100 mM sodium phosphate, pH 6.7) at 20 °C are very similar and indicate that both proteins have predominantly native structure (data not shown). The circular dichroism spectrum of 3SS-lysozyme under the initial unfolding conditions (4 M GdnHCl, 100 mM phosphate, pH 2.0) at 20 °C shows considerably less organized backbone structure, indicating that this species is denatured (data not shown). Aune and Tanford (1969) have demonstrated that unmodified lysozyme is also completely denatured under these unfolding conditions. These results indicate that both 3SS-lysozyme and unmodified lysozyme are unfolded at 4 M GdnHCl, pH 2, under the initial denaturing conditions and are folded at 0.5 M GdnHCl, pH 6.7, and 20 °C, the most denaturing final folding conditions used in the studies of 3SS-lysozyme. Previous work (Aune & Tanford, 1969; Greene & Pace, 1974; Ahmad & Bigelow, 1982) has demonstrated that unmodified lysozyme is folded under all of the final folding conditions used here.

Stopped-Flow Absorbance and Fluorescence Measurements. All measurements were carried out on a Hi-Tech Scientific preparative quench/stopped-flow spectrofluorimeter Model PQ/SF-53 instrument interfaced with a Keithley system 570 A/D converter. The temperature was controlled to ±0.1 °C by a Forma water bath equipped with a Pump Co. "Little Giant" pump to increase the rate of water circulation. 3SS-lysozyme or unmodified lysozyme was jumped from initial, unfolding conditions to final refolding conditions by a 1:10 dilution into the appropriate buffer. For the experiments carried out at pH 6.7, the initial unfolding buffer was 4 M GdnHCl and 100 mM phosphate, pH 2.0, and the final, refolding buffer was 100 mM phosphate with 0.15, 0.70, 1.25, or 1.80 M GdnHCl to yield the desired final GdnHCl concentration of 0.5, 1.0, 1.5, or 2.0 M, respectively. The pH of the refolding buffer was adjusted to between 7.0 and 7.1 so that the final pH after mixing was 6.7 in each case. For the pH 3.0 experiments, the initial unfolding buffer was 50 mM glycine and 4.5 M GdnHCl, pH 3.0, and the final folding buffer was 50 mM glycine and 0.5 M GdnHCl, pH 3.0. Syringes were driven pneumatically with a gas pressure of 3 bar. The dead time of the instrument has been calculated to be 2.1 ± 0.2 ms (Houry et al., 1994). Since this value is small compared to the time constants being measured, it was not taken into account in fitting the data.

For absorbance measurements, light generated by a 30-W deuterium lamp passed through a grating monochromator with a nominal dispersion of 7 nm/mm. The path length was 10 mm. Refolding kinetics were followed at 250, 292, and 301 nm. The protein concentration in the initial unfolding buffer ranged from 138 to 143 μM for unmodified lysozyme and from 107 to 156 μM for 3SS-lysozyme.

Fluorescence measurements were made using a 75-W xenon arc lamp. The excitation wavelength for all measurements was 280 nm with a slit width of 1 mm for unmodified lysozyme and 5 mm for 3SS-lysozyme, and the intrinsic fluorescence was monitored by using a 300–400 nm band pass filter. The excitation path length was 10 mm, and the emission path length was 2 mm. Initial protein concentrations used were 25.4 and 138 μM for unmodified lysozyme and 107 μM for 3SS-lysozyme.

Data Analysis. Data were fit to either a monophasic

$$A_\infty - A(t) = A_1 e^{-t/\tau_1} \quad (1)$$

or biphasic

$$A_\infty - A(t) = A_1 e^{-t/\tau_1} + A_2 e^{-t/\tau_2} \quad (2)$$

exponential model by using a nonlinear least-squares fitting procedure in which A_∞ and $A(t)$ are the observed absorbance (or fluorescence) of the protein at infinite time and at time t, respectively, after the solvent jump. A_1 and A_2 are the amplitudes of two exponential changes, and τ_1 and τ_2 are their kinetic time constants. The values of τ_1 and τ_2 are of different orders of magnitude; therefore, no corrections to the amplitudes were required to account for the sequential folding pathway.

Each experiment was repeated a minimum of three times (most were repeated 10 times), resulting in multiple data sets. Each data set was fit separately to eq 1 or 2 using the Levenberg–Marquardt algorithm (Press et al., 1990). All fits had a reduced χ^2 value of between 1.00 and 1.10, indicating that the data were well fit by eqs 1 and 2. Standard deviations were determined in the usual fashion by averaging over the data sets. All errors are given at the 95% confidence limit. In the case of the fluorescence data for unmodified lysozyme, the standard deviations were so small that additional data analysis was carried out to confirm the accuracy of the error analysis. While the small standard deviations found for the fluorescence data could be the result of the large amplitudes, i.e., the errors are small, they could also result from a systematic error in the fit. A significant systematic error in the fitting of the data could arise if the error for a single measurement was large but the reproducibility of the fit was high. To investigate this possibility, the shape of the χ^2 surface for individual data sets was determined. At 95% confidence, the uncertainties in each individual data set were less than those determined for all the data sets by averaging. Hence, no systematic error due to the fitting of the data has occurred. More details on the procedures used in this analysis can be found in Dodge et al. (1994).

RESULTS

Before presenting the data, it is important to emphasize that we are considering only the fast folding phases of lysozyme. A slow phase which is believed to result from proline isomerization has been observed in earlier studies (Kato et al., 1981). Only ~10% of the protein refolds through the slow phase. This phase corresponds to ~10% of the total absorbance change and makes a much smaller contribution to the fluorescence-detected refolding. Hence, it will have a negligible influence on the results presented here. In addition, it is necessary to mention that the refolding of unmodified lysozyme is best fit by a sequential model. Therefore, it is only the final of the three observed kinetic phases that corresponds to the formation of the final native form of the protein. The other two phases observed here correspond to the formation of intermediates. This view is supported by the data presented here as well as by other studies (Kato et al., 1981, 1982; Chaffotte et al., 1992; Radford et al., 1992) and will be discussed in greater detail in the Discussion section.

Another important point is that all of the fluorescence amplitudes reported here are normalized to the total fluorescence of the native protein under the final folding conditions. This value was determined directly from the refolding experiments and corrected for contributions from scattered light by base-line subtraction.

Fluorescence-Detected Refolding of Unmodified Lysozyme. A typical fluorescence-detected data set for the refolding of unmodified lysozyme in 0.5 M GdnHCl and 100 mM sodium phosphate, pH 6.7 at 15 °C, is shown in Figure 1. This figure

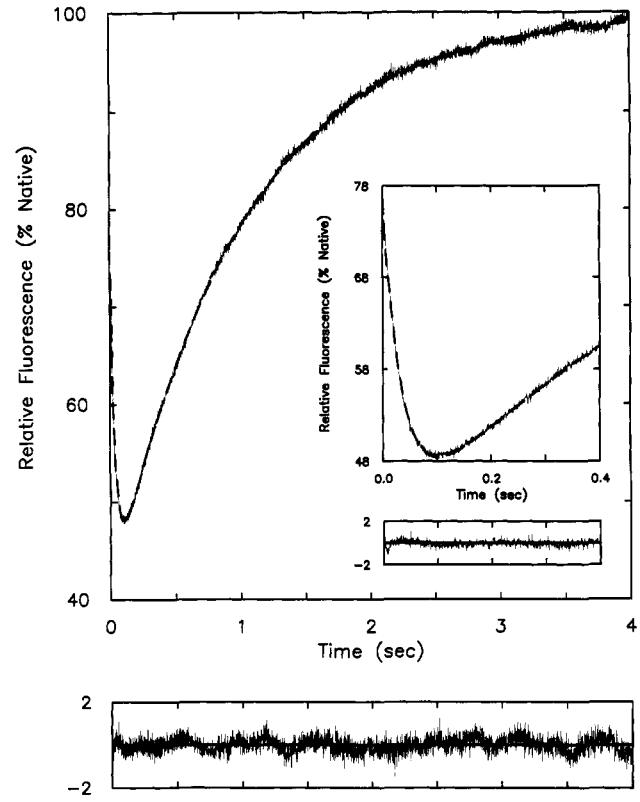

FIGURE 1: Typical data set showing the refolding of unmodified lysozyme monitored by fluorescence emission between 295 and 400 nm, 15 °C. The excitation wavelength was 280 nm. Refolding was achieved by a 10:1 stopped-flow dilution and pH jump from 4 M GdnHCl, pH 2.0, to 0.5 M GdnHCl, pH 6.7, in 100 mM sodium phosphate buffer. The final protein concentration was 12.5 μM. The inset shows a blowup of the early time regime. The lower panel shows the residuals, the difference between the data and the fitted function (dashed line). The fit of the calculated curve was judged by χ^2 analysis (χ^2= 1.03).

Table 1: Temperature Dependence of Kinetic Data for Fluorescence-Detected Refolding of Unmodified Lysozyme[a]

temp (°C)	hidden amplitude (%)[b]	τ_1 (ms)	amplitude of τ_1 (%)	τ_2 (s)	amplitude of τ_2 (%)
10	−38.9 ± 2.8[c]	67.6 ± 0.7	−41.2 ± 1.0	2.10 ± 0.01	59.9 ± 1.4
15	−44.9 ± 3.0	36.9 ± 0.7	−36.1 ± 1.1	1.01 ± 0.01	59.1 ± 1.7
20	−43.9 ± 3.0	20.0 ± 0.4	−30.6 ± 0.9	0.463 ± 0.003	56.8 ± 0.9

[a] Experimental conditions were as follows: Initial conditions: 4 M GdnHCl, pH 2; final conditions: 0.5 M GdnHCl, pH 6.7. [b] Amplitudes are normalized to the total fluorescence of the folded protein under the final folding conditions. A negative sign indicates that fluorescence quenching is occurring in that phase. [c] The error is calculated at the 95% confidence limit.

illustrates that the refolding is biphasic; the fluorescence is rapidly quenched in an initial phase (very-fast phase) and then slowly recovers in the final phase (fast phase). The amplitudes of both phases are very large, approximately 36% and 59% of the total fluorescence of the native unmodified protein for the very-fast and fast fluorescence phases, respectively. The amplitudes were obtained by fitting the data to a biexponential model (eq 2). There are no observable mixing artifacts in the fluorescence data.

The temperature dependence of the kinetic parameters obtained from the fluorescence-detected refolding measurements at 0.5 M GdnHCl is given in Table 1, and the dependence of those parameters on the GdnHCl concentration at 15 °C is given in Table 2. The time constant of the fast phase, denoted by τ_2, is observed to decrease as the temperature is increased. The time constant for the very-fast phase, τ_1, also

Table 2: Guanidine Dependence of Kinetic Data for Fluorescence-Detected Refolding of Unmodified Lysozyme[a]

final GdnHCl (M)	hidden amplitude (%)[b]	τ_1 (ms)	amplitude of τ_1 (%)	τ_2 (s)	amplitude of τ_2 (%)
0.5	−44.9 ± 3.0[c]	36.9 ± 0.7	−36.1 ± 1.1	1.01 ± 0.01	59.1 ± 1.7
1.0	−31.3 ± 2.1	59.2 ± 0.4	−48.1 ± 1.3	1.40 ± 0.02	55.9 ± 1.5
1.5	−20.4 ± 2.1	127 ± 2	−54.1 ± 0.9	1.97 ± 0.01	51.8 ± 1.0
2.0	−10.3 ± 2.1	263 ± 2	−44.5 ± 1.2	3.22 ± 0.04	33.2 ± 1.0

[a] Experimental conditions were as follows: Initial conditions: 4 M GdnHCl, pH 2; final conditions: pH 6.7, 15 °C. [b] Amplitudes are normalized to the total fluorescence of the folded protein under the final folding conditions. A negative sign indicates that fluorescence quenching is occurring in that phase. [c] The error is calculated at the 95% confidence limit.

Table 3: Relative Fluorescence Intensity of Unfolded Unmodified Lysozyme[a]

temp (°C)	final GdnHCl (M)	rel fluorescence intensity[b] (% native)	temp (°C)	final GdnHCl (M)	rel fluorescence intensity[b] (% native)
10	0.5	119.7 ± 1.3[c]	15	1.5	121.7 ± 2.6
15	0.5	122.0 ± 2.9	15	2.0	121.6 ± 2.5
20	0.5	117.8 ± 2.6	25[d]	1.0	143.5 ± 6.7
15	1.0	123.5 ± 2.5			

[a] Except where noted, initial unfolding conditions were 4 M GdnHCl, pH 2.0. pH of final folding conditions was 6.7. [b] Fluorescence intensity of unmodified lysozyme under initial, unfolding conditions expressed as the % of lysozyme fluorescence under final, folding conditions. [c] The error is calculated at the 95% confidence limit. [d] Initial unfolding conditions were 4.5 M GdnHCl, pH 3.0. pH under final folding conditions was 3.0.

decreases with increasing temperature. The amplitude for the fast phase is temperature independent, while the amplitude of the very-fast phase decreases with increasing temperature.

The fluorescence refolding data for unmodified lysozyme also reveal the presence of a hidden phase that occurs during the dead time of the stopped-flow instrument, which is approximately 2 ms (Houry et al., 1994). The amplitude of this phase was determined by measuring the fluorescence of unfolded unmodified lysozyme in the unfolding buffer relative to the folded protein; these values are listed in Table 3. Therefore, from Table 3, under the conditions used in obtaining the data of Figure 1, the relative fluorescence of the unfolded protein is 122% that of the native protein. It can be seen in Figure 1 that, at the earliest observable time point, the fluorescence intensity is between 75% and 80% of that of the native protein, indicating the existence of a large hidden or "burst" phase that occurs in the dead time of the instrument. The amplitude of this burst phase under the various folding conditions (temperature and GdnHCl concentrations) at pH 6.7 is shown in the second column of Tables 1 and 2.

Within the experimental error, the amplitude of the burst phase at 0.5 M GdnHCl exhibits no temperature dependence. Moreover, the sum of the amplitude of the burst phase and the amplitude of the very fast phase is, within the experimental error, also temperature invariant.

In contrast to the temperature dependence at 0.5 M GdnHCl, the dependence on the final GdnHCl concentration of the fluorescence amplitudes of all three phases at 15 °C is large. As shown in Table 2, the burst phase amplitude shows a large linear decrease in the magnitude of its amplitude, from 45% to 10%, as the final GdnHCl concentration increases from 0.5 to 2.0 M. The fast phase shows a small decrease in amplitude as the final GdnHCl concentration increases from 0.5 to 1.5 M, but when the GdnHCl is increased to 2.0 M, the amplitude drops to 33% (as compared to 59% at 0.5 M GdnHCl). In contrast to the other phases, the amplitude of the very-fast phase increases as the GdnHCl concentration is raised from 0.5 to 1.5 M, but decreases when the GdnHCl concentration is raised to 2.0 M. While the amplitudes of the very-fast phase and of the burst phase undergo large changes as a function of the GdnHCl concentration, the sum of their amplitudes remains constant from 0.5 to 1.5 M GdnHCl and the very-fast phase continues to be a single-exponential process; i.e., there is no evidence of biphasic behavior in the very-fast phase. Possible explanations for this behavior will be presented in the Discussion section.

The time constants for the fast and very-fast phases increase as the concentration of GdnHCl increases. The value of τ_1 exhibits the larger dependence on the GdnHCl concentration, increasing by a factor of 7 over the range of 0.5–2.0 M in the GdnHCl concentration as compared to the 3-fold increase in τ_2 over the same range.

The concentration dependence of the fluorescence experiments at pH 6.7 was determined by carrying out the studies at two final folding protein concentrations (2.3 and 12.5 μM). There was no difference within experimental error between the results obtained at the two different protein concentrations.

Relative Fluorescence Intensity of Unmodified Lysozyme. The fluorescence intensities of the unfolded protein relative to that of the native protein for unmodified lysozyme under each of the final folding conditions are presented in Table 3. These values were determined from direct fluorescence measurements on the stopped-flow instrument under the same conditions used in the refolding experiments. Because the extinction coefficient of lysozyme at 280 nm is insensitive to the conformation of the protein (Denton & Scheraga, 1991), the relative fluorescence which is what is actually measured is equivalent to the relative quantum yield. These results demonstrate that, when refolding is carried out at pH 6.7, the quantum yield of the unfolded protein under unfolding conditions is approximately 120% that of the refolded protein in folding conditions. Because the unfolding conditions are the same in all of the experiments carried out at pH 6.7, this indicates that the quantum yield of unmodified lysozyme in the various folding buffers at pH 6.7 is also constant. Given the absence of any temperature or GdnHCl dependence at pH 6.7, the comparatively large, 143%, relative quantum yield of unmodified lysozyme in the unfolded compared to the folded state at pH 3, 25 °C, probably results from the lower pH of the final folding solution, pH 3, rather than the higher temperature, 25 °C.

Absorbance-Detected Refolding of Unmodified Lysozyme. Figure 2 shows a refolding data set for unmodified lysozyme observed by absorbance at 250 nm when the protein is refolded at 15 °C, 0.5 M GdnHCl, 100 mM phosphate, and pH 6.7 (the same solution conditions as in Figure 1). Lysozyme demonstrates a characteristic increase in absorbance upon refolding when monitored at this wavelength. Of particular interest is the region of the curve corresponding to the earliest time points (see inset of Figure 2) which illustrates the biphasic nature of the folding process in this time regime. The absorbance refolding data for unmodified lysozyme were best fit by a biexponential equation (eq. 2). Table 4 lists the kinetic parameters for the temperature dependence of the absorbance-detected kinetics at a final GdnHCl concentration of 0.5 M, and Table 5 lists the dependence of those parameters on the final GdnHCl concentration at 15 °C. Unlike the fluorescence data, the absorbance data exhibited small temperature-dependent mixing artifacts. This is primarily due to the much smaller absolute amplitudes of the absorbance-detected

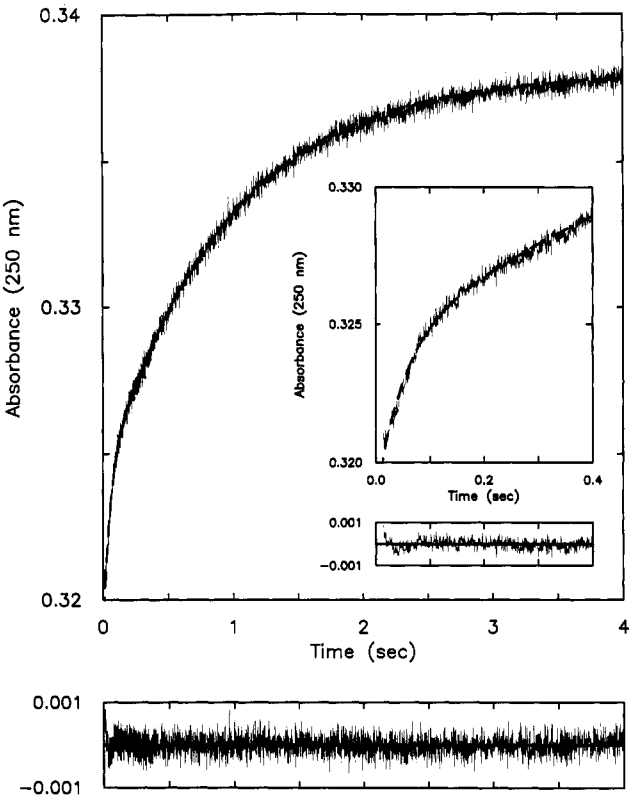

FIGURE 2: Typical data set showing the refolding of unmodified lysozyme monitored by absorbance (observed OD) at 250 nm, 15 °C. χ^2= 1.01. All other information is as described in Figure 1.

Table 4: Temperature Dependence of Kinetic Data for Absorbance-Detected Refolding of Unmodified Lysozyme[a]

temp (°C)	wavelength (nm)	τ_1 (ms)	amplitude of τ_1 (M^{-1} cm^{-1})	τ_2 (s)	amplitude of τ_2 (M^{-1} cm^{-1})
10	250	84.0 ± 16.4[b]	4.04 ± 1.10	2.02 ± 0.11[b]	10.8 ± 0.5
10	292	ND[c]	ND	2.02 ± 0.06	−7.18 ± 0.20
15	250	36.7 ± 8.6	3.53 ± 1.26	1.00 ± 0.03	10.3 ± 0.4
15	292	ND	ND	0.938 ± 0.023	−7.44 ± 0.31
20	250	ND	ND	0.474 ± 0.015	10.8 ± 0.3
20	292	ND	ND	0.460 ± 0.019	−7.61 ± 0.30

[a] Experimental conditions were as follows: Initial conditions: 4 M GdnHCl, pH 2; final conditions: 0.5 M GdnHCl, pH 6.7. [b] The error is calculated at the 95% confidence limit. [c] ND indicates that the information could not be determined.

Table 5: Guanidine Dependence of Kinetic Data for Absorbance-Detected Refolding of Unmodified Lysozyme[a]

wavelength (nm)	final GdnHCl (M)	τ_1 (ms)	amplitude of τ_1 (M^{-1} cm^{-1})	τ_2 (s)	amplitude of τ_2 (M^{-1} cm^{-1})
250	0.5	36.7 ± 8.6[b]	3.53 ± 1.26	1.00 ± 0.03	10.3 ± 0.4
292	0.5	ND[c]	ND	0.938 ± 0.023	−7.44 ± 0.31
250	1.0	71.8 ± 10.6	5.01 ± 1.02	1.46 ± 0.04	12.1 ± 0.3
292	1.0	59.6 ± 20.0	2.93 ± 0.94	1.43 ± 0.04	−5.58 ± 0.37
250	2.0	289 ± 24	4.25 ± 0.21	3.27 ± 0.01	14.5 ± 0.5
292	2.0	285 ± 27	3.19 ± 0.32	3.24 ± 0.13	−3.24 ± 0.23

[a] Experimental conditions were as follows: Initial conditions: 4 M GdnHCl, pH 2; final conditions: pH 6.7, 15 °C. [b] The error is calculated at the 95% confidence limit. [c] ND indicates that the information could not be determined.

refolding phases. The major mixing artifacts are complete within 8–12 ms, and data obtained prior to 12 ms were excluded from all data sets prior to fitting. In addition, small base-line ripples extended for up to 60 ms following the initiation of refolding. While these ripples were for the most part small with respect to the data taken at 250 nm (the wavelength at which the largest amplitude of refolding was observed), they interfered with the analysis of data acquired at 292 nm. Therefore, for data acquired at 292 nm which could not be fit to a biexponential expression because of the mixing artifacts, the first 500 ms of data were removed and the remaining data were fit to a monoexponential equation. Although there are differences between the data reported for the two wavelengths with regard to the sign and magnitude of the folding amplitudes, the time constants agree within the experimental error for each set of final folding conditions studied. The values for the time constants determined by absorbance agree well with those obtained from the fluorescence measurements (Tables 1 and 2), suggesting that the same process is observed both by absorbance and by fluorescence.

Table 6: Kinetic Data for the Refolding of Unmodified Lysozyme at Low pH[a]

method of detection	hidden amplitude	τ (s)	amplitude of τ
fluorescence[b]	−38.8 ± 6.2[c]	1.14 ± 0.09	−4.69 ± 0.40
absorbance at 250 nm[d]		1.04 ± 0.04	15.0 ± 1.0
absorbance at 292 nm[d]		1.02 ± 0.15	−3.33 ± 0.64

[a] Experimental conditions were as follows: Initial conditions: 4.5 M GdnHCl, pH 3.0, 25 °C; final conditions: 1 M GdnHCl. [b] Amplitudes are normalized to the total fluorescence of the folded protein under the final folding conditions. A negative sign indicates that fluorescence quenching is occurring in that phase. [c] The error is calculated at the 95% confidence limit. [d] Absorbance amplitudes are expressed in units of M^{-1} cm^{-1}.

In contrast to the fluorescence-detected refolding, there is no apparent temperature dependence of the magnitude of the absorbance amplitudes (at 250 and 292 nm) observed for either the very-fast or fast phases at 0.5 M GdnHCl. There is also no dependence (within the experimental error) of the amplitude of the very-fast phase with increasing GdnHCl concentrations at 15 °C. However, the amplitude of the fast phase at 250 nm increases with increasing GdnHCl concentration, and at 292 nm it decreases.

Measurements were also made at 301 nm (data not shown), and the τ values obtained were in good agreement with those determined at 250 and 292 nm. The observed amplitudes at 301 nm were smaller than those at the other wavelengths, resulting in a lower signal-to-noise ratio and consequently greater interference from mixing artifacts.

It is important to emphasize that the absorbance amplitudes were considerably smaller than the fluorescence amplitudes. This fact is clearly evident from the much smaller standard deviations of the fluorescence data relative to the absorbance-detected results. Given the excellent agreement between the τ values measured by the two techniques, i.e., they appear to be monitoring the same processes, further analysis of the data is best accomplished by using the results determined from the fluorescence-detected data since uncertainties in the kinetic quantities are much smaller.

Studies of Unmodified Lysozyme at Low pH. Table 6 lists the absorbance- and fluorescence-detected refolding results obtained at pH 3.0, 1.0 M GdnHCl, and 25 °C. The refolding process, unlike that at pH 6.7, is a monoexponential process. The fluorescence amplitude of this single phase is an order of magnitude smaller than the final folding phase observed at pH 6.7. The hidden amplitude is approximately the same as that measured when refolding is carried out at the higher pH.

Refolding of 3SS-Lysozyme. Figure 3 shows the absorbance-detected refolding of 3SS-lysozyme observed at 250 nm when the protein is refolded at 15 °C, 0.5 M GdnHCl, 100 mM sodium phosphate, and pH 6.7 (the same solution

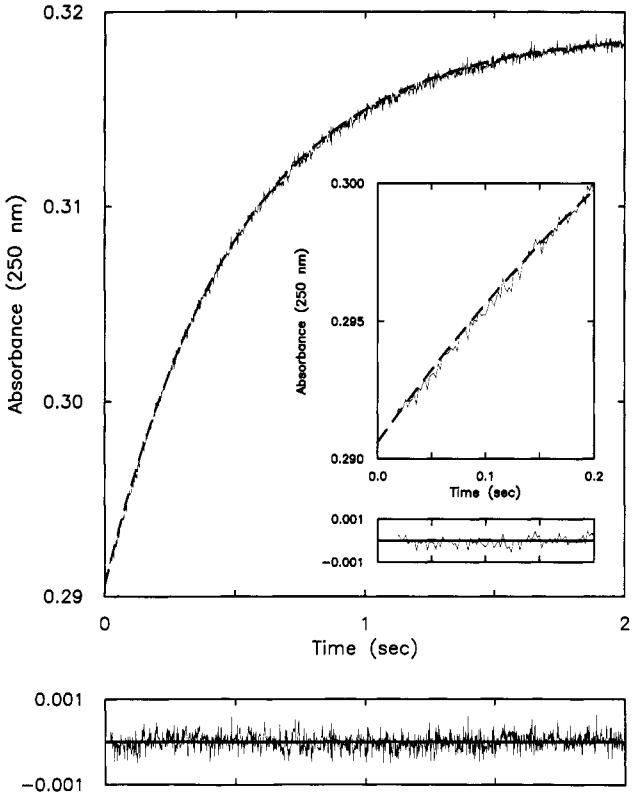

FIGURE 3: Typical data set showing the refolding of 3SS-lysozyme monitored by absorbance (observed OD) at 250 nm, 15 °C. The final protein concentration was 14.2 μM. χ^2= 1.04. All other information is as described in Figure 1.

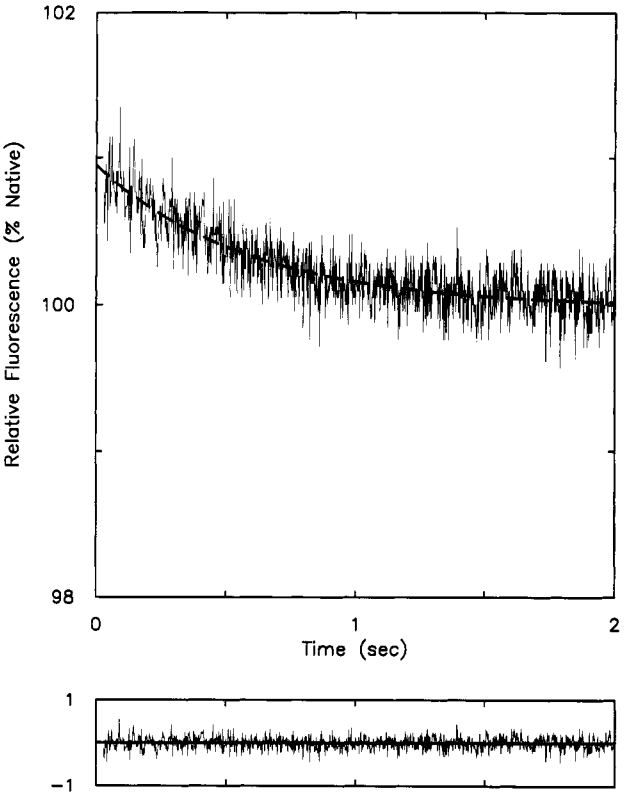

FIGURE 4: Typical data set showing the refolding of 3SS-lysozyme monitored by fluorescence at 15 °C. The final protein concentration was 9.7 μM. χ^2 = 1.02. All other information is as described in Figure 1.

Table 7: Kinetic Data for Absorbance-Detected Refolding of 3SS-Lysozyme[a]

temp (°C)	wavelength (nm)	τ (s)	amplitude (M^{-1} cm^{-1})
10	250	0.834 ± 0.043[b]	16.7 ± 1.4
15	250	0.514 ± 0.007	18.0 ± 1.1
15	292	0.493 ± 0.039	−2.30 ± 0.93
20	250	0.331 ± 0.051	16.2 ± 2.1

[a] Experimental conditions were as follows: Initial conditions: 4 M GdnHCl, pH 2; final conditions: 0.5 M GdnHCl, pH 6.7. [b] The error is calculated at the 95% confidence limit.

Table 8: Kinetic Data for Fluorescence-Detected Refolding of 3SS-Lysozyme[a]

temp (°C)	τ (s)	amplitude (%)[b]
10	0.670 ± 0.10[c]	1.54 ± 0.24
15	0.518 ± 0.079	−0.99 ± 0.13
20	0.320 ± 0.013	−4.36 ± 0.60

[a] Experimental conditions were as follows: Initial conditions: 4 M GdnHCl, pH 2; final conditions: 0.5 M GdnHCl, pH 6.7. [b] Amplitudes are normalized to the total fluorescence of the folded protein under the final folding conditions. A negative sign indicates that fluorescence quenching is occurring in that phase. [c] The error is calculated at the 95% confidence limit.

conditions as in Figures 1 and 2). In contrast to the early folding process for unmodified lysozyme shown in Figure 2 (compare inset in Figure 3 to inset in Figure 2), the data for 3SS-lysozyme are best fit by a single-exponential equation. The effect of temperature on the time constant and amplitude of this single phase is shown in Table 7. The time constant, τ, decreases by 35–40% with each 5 °C increase in temperature, while the total amplitude observed at 250 nm remains unchanged. Of the greatest interest, however, is the fact that, at each temperature, τ for 3SS-lysozyme is less than τ_2 for the folding of unmodified lysozyme. Hence, 3SS-lysozyme refolds *more* rapidly than the unmodified protein under these conditions.

A typical data set for the fluorescence-detected refolding of 3SS-lysozyme at 0.5 M GdnHCl at 20 °C is shown in Figure 4. The most noteworthy feature of this data set is the absence of a substantial change in amplitude upon refolding. These data, like the absorbance-detected refolding data for 3SS-lysozyme, are best fit by a single-exponential expression. As was the case for the unmodified protein, the values for the time constants determined from the fluorescence measurements, reported as τ in Table 8, are in good agreement with those determined from the absorbance measurements. These results reiterate the fact that 3SS-lysozyme folds faster in the temperature range of 10–20 °C than the unmodified protein.

In contrast to the unmodified protein, the absorbance-detected kinetic data are more accurate than the fluorescence-detected data. This arises primarily from the very small amplitude of the fluorescent phase, although the amplitudes at 250 nm are larger for 3SS-lysozyme than for either of the phases observed for the unmodified protein. Hence, further analysis of the data for 3SS-lysozyme will be carried out with the absorbance results.

Activation Enthalpies. The activation enthalpies for the refolding processes measured at a final GdnHCl concentration of 0.5 M were calculated from the temperature dependence of the time constants. For the reasons given above, the activation enthalpies for the unmodified protein were calculated using the fluorescence data given in Table 1, while for 3SS-lysozyme the absorbance-detected data given in Table 7 were used.

The activation enthalpy for the very-fast phase of unmodified lysozyme is 20.0 ± 1.5 kcal/mol. The activation enthalpy for the fast phase of unmodified lysozyme is 24.8 ± 1.1 kcal/mol.

The activation enthalpy for the single refolding phase of 3SS-lysozyme is 15.2 ± 4.7 kcal/mol. All errors are expressed at the 95% confidence limit.

DISCUSSION

As presented in the introductory section, there have already been many significant studies carried out on the folding of unmodified lysozyme. This study augments these previous studies both by employing another detection method, intrinsic fluorescence, and in the use of a derivative, 3SS-lysozyme, with which to probe the contribution of the 6–127 disulfide bond to the folding process of lysozyme. The data presented here demonstrate that unmodified lysozyme exhibits two fast phases upon refolding when monitored by absorbance or fluorescence. The slower of these two fast phases appears to correspond to that identified by earlier workers (Kato et al., 1982) as corresponding to the formation of the final correctly folded native protein. The very-fast phase has not been observed previously by absorbance-detected refolding although its existence was suggested by earlier workers (Kato et al., 1981).

Clearly, one of the most significant results presented here is the presence of unusually large amplitudes observed during the fluorescence-detected refolding of unmodified lysozyme. We will draw upon the considerable body of pre-existing data to arrive at the most plausible explanations of the structural origins of the large fluorescence-detected phases that we observe. These will be developed in the following sections. In addition, folding mechanisms will be proposed to explain the difference in the refolding properties of unmodified lysozyme and 3SS-lysozyme.

Before carrying out comparisons between our studies and those in other laboratories, it is important to recognize that many of these experiments have been carried out under different solution conditions, i.e., denaturant concentration, pH, and temperature. It must be stressed that any attempt to relate behavior under different solution conditions by a comparison of the rates of formation of the native protein is unwarranted, since the temperature, denaturant, and pH dependence of each phase is likely be different. This is evident in our own data for unmodified lysozyme where, at 0.5 M GdnHCl, 10 °C, and at 1.5 M GdnHCl, 15 °C, the native protein forms with a time constant of ~2 s, while the time constants for the very-fast phase differ by a factor of ~2 as do the burst phase amplitudes.

Another important consideration that must be addressed is that each method determines the extent of folding by monitoring *different* probes. There is a fundamental difference in what is defined as structure by optical measurements and by H/D-exchange studies. Absorbance-, fluorescence-, and CD-monitored experiments measure a weight-averaged sum of the signals provided by *all* species in a mixture. H/D-exchange studies detect only stable structure, i.e., structure that is stable to exchange at elevated pH (9 or greater). For example, if two helical species are in rapid equilibrium with each other, only those amide protons that are protected in both species would be observed by H/D-exchange studies, indicating less secondary structure than would be determined by CD measurements.

Furthermore, optically-detected refolding is carried out by a single-jump experiment from unfolding to refolding conditions. In the case of H/D-exchange studies, the protein is first jumped from unfolding to refolding conditions, where, after a variable delay, it is jumped to high pH and subjected to a labeling pulse before being jumped back to low pH. As a consequence of this triple-jump procedure, and given that the duration of the labeling pulse is typically on the order of 10 ms, there will be considerable uncertainty in the determination of the zero time point. In the case of very rapid processes (when the time constant is within an order of magnitude of the uncertainty in the zero time point), this could result in situations in which time constants and amplitudes obtained from H/D-exchange folding studies cannot be compared directly to time constants measured by other methods.

For all of these reasons, it is impractical to correlate processes measured by different techniques and under different solution conditions based solely on comparison of time constants. Therefore, in order to compare our refolding data to those obtained in previous studies of unmodified lysozyme, we will divide the kinetic phases into three groupings, burst phase, very-fast phase, and fast phase, in accordance with our fluorescence data for unmodified lysozyme. In comparison with the H/D-exchange studies, the assignments are somewhat arbitrary, but we have chosen to assign the initial protection that occurs in the first 10 ms to the burst phase, the protection of the α-helical regions of the protein (α-domain) to the very-fast phase, and the protection of the β-domain (with formation of the final native structure) to the fast phase. These comparisons will be used in subsequent sections to develop a detailed picture of the folding processes of unmodified lysozyme.

Fluorescence Properties of Unmodified Lysozyme. In order to interpret correctly the structural origins of the unusually large fluorescence amplitudes observed during refolding, the fluorescence properties of the separate unfolded and refolded states of unmodified lysozyme must first be considered. Lysozyme contains 6 tryptophan and 3 tyrosine residues. The tyrosines play little role in the fluorescence of the native protein under the solution conditions being considered here, either through a direct fluorescence contribution or through energy transfer to tryptophan (Imoto et al., 1972a,b) and, therefore, will not be considered further. The quantum yield of the native protein, when excited under the conditions that we have used in this study (280–285 nm), is ~30% (Lehrer & Fasman, 1967; Teichberg & Sharon, 1970) of the quantum yield expected for free tryptophan. This indicates that significant quenching of tryptophans occurs in the native state. The quantum yield of the GdnHCl-denatured state has been found to be within ~25% of that of the native protein (Imoto et al., 1972b), in agreement with the results at pH 6.7 that we have presented here (Table 3). At first, this would suggest that the quenching of tryptophan fluorescence that occurs in the native protein arises from sequence-specific and not structurally-specific processes. However, experiments evaluating the contribution of individual tryptophan residues to the fluorescence properties of lysozyme determined through the use of oxidized derivatives of lysozyme (Teichberg & Sharon, 1970; Imoto et al., 1972a,b; Formoso & Forster, 1975; Kuramitsu et al., 1978; Fukunaga et al., 1982; Yamasaki et al., 1990) and mutants (Kumagai et al., 1992) suggest otherwise.

These studies suggest that two residues, Trp-62 and Trp-108, account for 80–90% of the fluorescence of native lysozyme (Imoto et al., 1972a,b) but for only ~50% of the fluorescence in the GdnHCl-denatured state (pH 5.0, 5 M GdnHCl) (Imoto et al., 1972b). Fluorescence lifetime studies (Formoso & Forster, 1975) and quenching and denaturation studies (Imoto et al., 1972a) are consistent with these results. The individual contributions of these two residues to the fluorescence of native

lysozyme have been measured as 35–75% for Trp-62 (Imoto et al., 1972a,b; Fukunaga et al., 1982; Yamasaki et al., 1990; Kumagai et al., 1992) and 45–65% for Trp-108 (Teichberg & Sharon, 1970; Imoto et al., 1972a,b; Kuramitsu et al., 1978). The precise contribution of these two tryptophans to the fluorescence of the native state is complicated since there is considerable evidence that energy transfer occurs between them (Imoto et al., 1972b; Formoso & Forster, 1975; Kuramitsu et al., 1978).

These data suggest that the remaining tryptophan residues (28, 63, 111, and 123) make little contribution to the fluorescence of the native protein and that they are considerably more quenched in the native state than in the GdnHCl-denatured state. Therefore, on the basis of these results, Trp-28, -63, -111, and -123 should contribute a negative amplitude of ~40% (relative to the fluorescence of the native protein) during the fluorescence-detected refolding of lysozyme. Both the solvent effects resulting from the decrease in the concentration of GdnHCl under folding conditions and the formation of native structure contribute to this negative amplitude.

It must be mentioned that, given the proximity of Trp-62 and Trp-63 in the protein, the possibility exists that some of the fluorescence properties assigned to Trp-62 could arise from interactions with Trp-63. However, to simplify the discussion that follows, this possible contribution will be neglected. This in no way affects the analysis that follows.

The Burst Phase. The change in the far-UV CD spectrum that occurs during the burst phase (first 4 ms) suggests that 100% of the native secondary structure has formed (Chaffotte et al., 1992) while, by NMR spectroscopy, only ~40% of the amide protons in the α-domain and ~24% of the amide protons in the β-domain are protected in the first 10 ms (Radford et al., 1992). Taken together, these results suggest that much of the structure formed in the burst phase is still in rapid equilibrium with the denatured state. Since Trp-28, -63, -111, and -123 are significantly more quenched in their native state as discussed above, and since Trp-28, -111, and -123 are found in regions of organized helical structure, much of the observed fluorescence decrease (relative to the native protein) that we observe in the burst phase could arise simply from the formation of the native helical structure around those three tryptophans. Such a conclusion is consistent with the results of the H/D-exchange and the CD-detected refolding studies.

As stated above, part of the burst phase amplitude probably arises from the change in solution conditions upon refolding. The GdnHCl dependence of tryptophan fluorescence has been observed in model compounds to be very small (Edelhoch & Lippoldt, 1969; Kronman & Holmes, 1971) and is in general linear, as indicated by its use in determining denaturation base lines in GdnHCl-denaturation curves of proteins including hen egg white (Inoue et al., 1992) and human (Herning et al., 1991) lysozymes. Therefore, given that the amplitude of the burst phase at 2 M GdnHCl is only ~10% (Table 2), we would expect that the pH and guanidine effects at 0.5 M GdnHCl probably account for substantially less than half of the observed 45% amplitude (Table 2). Consequently, the decrease of the burst phase amplitude with increasing GdnHCl concentration (Table 2) suggests that the structure formed in the burst phase becomes denatured at higher GdnHCl concentrations. These data are consistent with the suggestion, made from a comparison of the H/D-exchange and CD studies, that much of the structure is metastable.

The Very-Fast and Fast Phases. The very-fast fluorescence-detected phase results in the population of an intermediate with highly quenched fluorescence followed by a slow recovery of fluorescence (the fast phase). This intermediate state appears to correspond (based on the time constant and pH dependence of formation as described in the next section) to the intermediate observed by Radford et al. (1992) and Chaffotte et al. (1992) in which the ellipticity in the far-UV CD (222 or 225 nm) is more negative than the corresponding ellipticity of native lysozyme. In the H/D-exchange studies, the intermediate formed following the burst phase involves the complete protection of amides in the α-domain and occurs with a time constant of ~60 ms, which would appear to be in reasonable agreement with the CD- and fluorescence-detected very-fast phases. However, Radford et al. (1992) have carried out CD studies under the same final folding conditions as the H/D-exchange studies and have observed that the change in the CD spectrum occurs faster under their conditions than does formation of the α-domain detected by H/D exchange. This difference suggests that there is a lag between the formation of the structure leading to the optically observed phase and the subsequent significant stabilization of that structure as reflected by the H/D-exchange studies. An alternative explanation is that the apparent lack of correlation between the CD and H/D-exchange results arises from the zero-time uncertainty of the triple-jump H/D-exchange measurement when compared to the single-jump CD experiment; i.e., the final folding conditions may be identical, but the experimental folding procedures are not the same. On the basis of the H/D-exchange studies, the very fast phase appears to correlate with the formation of the stabilized α-domain, the fast phase to the final stabilization of the β-domain.

While, considering solely the CD data, the origin of the very-fast phase at 222 nm is uncertain, the large amplitude of the fluorescence-detected very-fast phase clearly indicates the involvement of tryptophan. If we proceed on the simplest assumption that the quenching of the intermediate state formed through the very-fast phase is the result of a single tryptophan, then according to our knowledge of the fluorescence properties of lysozyme, as discussed above, the significantly quenched intermediate state that we observe probably results from quenching of either Trp-62 or Trp-108.

This leads to two simple explanations of the properties of the CD- and fluorescence-detected intermediate. The large negative ellipticity at 222 nm could involve a constraint on a disulfide bond as proposed by Chaffotte et al. (1992) and that disulfide could interact with either Trp-62 or Trp-108, which results in the highly quenched fluorescence. Alternatively, both the CD and fluorescence data can be explained by eliminating any consideration of disulfide bond strain; i.e., the anomalous far-UV CD may arise from one or more tryptophan residues and may not reflect any constraint on a disulfide bond. Although it was argued by Chaffotte et al. (1992) that the contribution of tryptophan in the far-UV region would be too small to account for the observed overshooting of the CD based on studies of tryptophan amide by Adler et al. (1973), contributions by tryptophan to the CD at 222 nm of proteins have been observed which are over 40 times larger (Arnold et al., 1992) than those observed by Adler et al. (1973). More importantly, CD studies of the Trp-108 derivatives, in which tryptophan has been changed to oxindole or oxindole ester (Teichberg et al., 1970; Tanaka et al., 1975), glutamine, or tyrosine (Inoue et al., 1992), show that the contribution of Trp-108 to the CD of native lysozyme is of the right magnitude to account for the observed overshooting of the CD at 222 nm.

Therefore, the simplest explanation is that the fluorescence, far-UV CD, and near-UV CD reflect a single process arising from a non-native tertiary interaction involving either Trp-62 or Trp-108. This could involve quenching by means of interactions with charged residues or disulfides, or it could result from a coupling of aromatic residues (ring stacking). Such interactions have been implicated in the large negative contribution to the 222 nm CD in fd bacteriophage (Arnold et al., 1992) as well as in fluorescence quenching in polypeptides (Longworth, 1966).

Studies at Low pH. Studies at pH 3.0 and 25 °C detected by both absorbance and fluorescence indicate that folding under these conditions is best represented by a monoexponential process. The fluorescence-detected burst phase, which is determined indirectly, is still present and comparable in amplitude to that measured at pH 6.7, 0.5 M GdnHCl, implying that a mechanism similar to that proposed for unmodified lysozyme at pH 6.7 occurs under these conditions, i.e., formation of native helical structure around Trp-28, -111, and -123. Chaffotte et al. (1992) have reported that, while significant secondary structure is formed during the burst phase, no overshoot in the far-UV CD is observed at acidic pH (pH 2). The fact that the fluorescence-quenched intermediate and the overshoot in the far-UV CD exhibit similar pH dependencies (in addition to the similar time constants for their formation) supports the assertion made earlier that the very-fast phase that we observe and the phase observed by Radford et al. (1992) and by Chaffotte et al. (1992), which involves an overshoot in the far-UV CD signal, arise from the same process.

There are two possible explanations for the absence of the very-fast phase (and the highly quenched intermediate) at pH 3. The first is that the pathway has not changed, viz., the absence of the very-fast phase is a consequence of the titration of a carboxyl side chain, and that at neutral pH it is the interaction between the charged carboxylate group and a tryptophan side chain that is responsible for the observation of the large fluorescence-quenched phase. The second possibility is that the folding pathway(s) at these pH's are substantially different. One such possibility is that the lower pH destabilizes the α-domain, making the refolding pathway of the unmodified protein at low pH similar to that of 3SS-lysozyme, as discussed in the following subsection. Our data cannot distinguish between these possibilities.

Dependence of Refolding on the Guanidine Concentration. As the concentration of GdnHCl is increased from 0.5 to 1.5 M, the amplitude of the burst phase decreases from 45% to 20% (Table 2). By contrast, over this same range of GdnHCl concentrations, the amplitude of the very-fast phase increases such that the sum of its amplitude and that of the burst phase remains constant. Furthermore, the very-fast phase remains a single-exponential process. This suggests that any structure that is denatured by GdnHCl in the burst phase is stabilized by whatever interactions are formed in the highly quenched intermediate. Such an explanation is inconsistent with the structural origin of the highly quenched intermediate arising from formation of correct secondary structure in the absence of tertiary contacts and strongly suggests that the correct interpretation (which also agrees better with the H/D-exchange studies) is that the α-domain is stabilized through the formation of non-native tertiary interactions which must be disrupted in order for the correct formation of the β-domain to occur.

Further insight into the folding mechanism can be obtained by an analysis of the dependence of the refolding process on

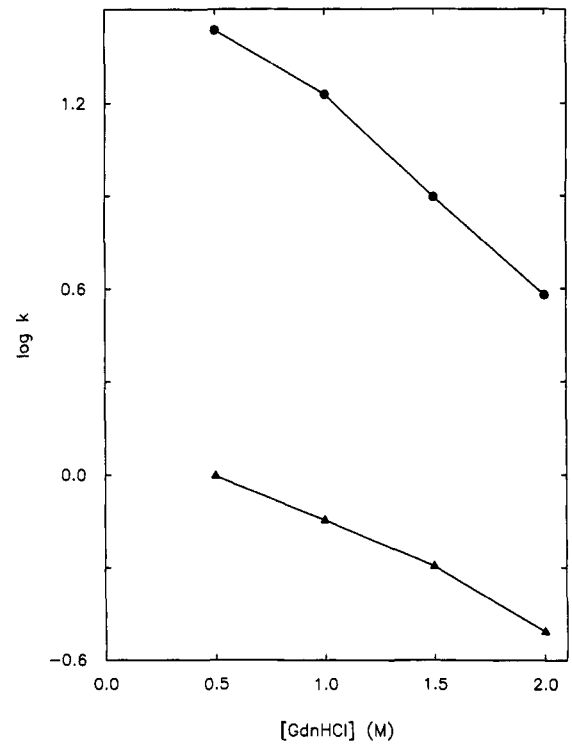

FIGURE 5: Plot of log k vs GdnHCl concentration at 15 °C, pH 6.7, for refolding of unmodified lysozyme. Rate constants, k, are obtained from fluorescence data given in Table 2. (●) Very-fast phase; (▲) fast phase.

the GdnHCl concentration. The relationship between the free energy of activation, $\Delta G^{\ddagger}$, and the denaturant concentration can be written as follows (Tanford, 1968; Schellman, 1978; Kuwajima et al., 1989; Matouschek et al., 1989):

$$\Delta G^{\ddagger} = \Delta G^{\ddagger}_{H_2O} - A[\text{GdnHCl}] \quad (3)$$

where $\Delta G^{\ddagger}_{H_2O}$ is the free energy of activation in the absence of denaturant, and A is a constant which is proportional to the difference in the exposed surface area of the transition state and the exposed surface area of the ground state species preceding the transition state. Because exposure of surface area decreases as the protein folds, values of A will be negative when considering a folding reaction. A more convenient form of eq 3 is to rewrite $\Delta G^{\ddagger}$ in terms of the rate constant, k.

$$\log k = \log k_{H_2O} + \frac{A}{2.303RT}[\text{GdnHCl}] \quad (4)$$

Figure 5 shows plots of log k vs GdnHCl concentration for the very-fast and fast phases at 15 °C using the fluorescence-detected rate constants (since the errors are sufficiently small to permit accurate determination of any deviations from linearity; error limits at 95% confidence are smaller than the symbols used in Figure 5). As can be seen in Figure 5, the very-fast phase rate constant displays a linear dependence from 1.0 to 2.0 M final GdnHCl concentration. The slope, however, is smaller from 0.5 to 1.0 M GdnHCl than from 1.0 to 2.0 M GdnHCl, suggesting either that, at the lower GdnHCl concentrations, the transition state is less compact than at the higher GdnHCl concentrations or that the intermediate(s) formed in the burst phase is more compact at lower GdnHCl concentration. The latter explanation is consistent with the observed decrease in the amplitude of the burst phase with increasing GdnHCl concentrations; i.e., there is less α-helical

structure formed during the burst phase at higher GdnHCl concentrations.

The plot of log k vs GdnHCl concentration for the fast phase is linear from 0.5 to 1.5 M GdnHCl but becomes steeper from 1.5 to 2.0 M GdnHCl. This indicates either that the transition state for formation of the β-domain becomes more compact at the higher GdnHCl concentrations or that the highly quenched intermediate formed in the very-fast phase is less compact at high GdnHCl concentrations. The latter explanation is consistent with the large decrease in the amplitude of the very-fast phase at 2 M GdnHCl, which suggests either a change in the contacts of the non-native interaction or that some portions of the α-domain have been destabilized. An additional possibility is that the folding pathway has changed and that only ~60% (based on the values in Table 2) of the protein folds through the pathway populated at lower GdnHCl concentrations. It is important to reiterate that the quantum yield of the native protein does not change within the experimental error (~2%) over the range of GdnHCl concentrations studied (Table 3); thus, the decrease in the fast phase amplitude at 2 M GdnHCl reflects a change in the fluorescence properties of the intermediate state(s) and not of the native protein.

It should also be noted that the magnitude of the value of A (the slopes of the lines in Figure 5) is significantly smaller for the fast phase than for the very-fast phase, which, in conjunction with the data discussed above, suggests that the protein becomes more compact after formation of the α-domain.

Refolding of 3SS-Lysozyme. The three-disulfide form of lysozyme folds without the appearance of any large change in the fluorescence-detected refolding or any biphasic behavior in either the absorbance- or fluorescence-detected refolding. This is in sharp contrast to the refolding of unmodified lysozyme, and there are several possible explanations for these differences. The most obvious one is that the same folding pathway is followed by both proteins and that the absence of the 6–127 disulfide bond removes a constraint (the same constraint that gives rise to the unusual far-UV and fluorescence-detected refolding properties). Alternatively, in the absence of the 6–127 disulfide bond, secondary structure may be only metastable until the formation of long-range, tertiary contacts. In this case, the three-disulfide derivative folds through a pathway that is different from that observed for native lysozyme.

It must be stressed that, even if the two proteins have different folding pathways, the folding pathway of 3SS-lysozyme could also be accessible to the unmodified protein. Since, as discussed above, H/D-exchange experiments (Radford et al., 1992) indicate that the native protein refolds with the formation of a heterogeneous population of intermediates, the intermediates populated during the refolding of 3SS-lysozyme could be present in the ensemble of folding intermediates of the unmodified protein. From this argument, it therefore follows that the removal of the 6–127 disulfide bond would shift the equilibrium distribution that occurs in the folding ensemble of the unmodified protein, presumably toward a less compact state with less stable secondary structure. There is some precedent in the literature for this interpretation. Much of the compact nature of a denatured protein is known to arise from the presence of disulfide bonds (Tanford, 1968). Theoretical studies suggest that a compact state favors the formation of organized secondary structure (Chan & Dill, 1990; Hao et al., 1992, 1993), α-helical structure in particular (Gregoret & Cohen, 1991). Furthermore, CD studies of partially and fully reduced forms of lysozyme demonstrate that the disulfide bonds are necessary for the formation of secondary structure, particularly α-helical structure (White, 1982).

Overall Folding Mechanism. Using the new information obtained here, a more complete picture of the folding pathway of unmodified lysozyme can be developed which is consistent with all of the existing data. The results presented here, interpreted in conjunction with other literature data, suggest that lysozyme refolds through an intermediate in which the α-domain is greatly stabilized by the formation of non-native tertiary interactions. The subsequent disruption of these non-native interactions is required for the formation of the correct tertiary contacts in the β-domain. Such a mechanism is inconsistent with the formation of the correct β-domain secondary structure in the first 4 ms of folding as suggested by the CD studies of Chaffotte et al. (1992) and would seem to indicate [as do the H/D-exchange studies of Radford et al. (1992) and, more importantly, inhibitor binding measurements (Dobson et al., 1994)] that the correct final native β-structure does not form until after the stabilization of the α-domain.

The level of fluorescence quenching observed in the intermediate containing the non-native tertiary interaction-(s) is too large to represent only a fraction of the protein and strongly indicates that all (or the vast majority) of the protein molecules contain this non-native interaction(s). Therefore, the multiple pathways proposed by Radford et al. (1992) must to some extent converge at the point at which the non-native tertiary interaction(s) occurs and formation of the α-domain is completed. Following formation of the α-domain, Radford et al. (1992) noted that amide protection occurs at different rates at various locations in the β-domain, an observation which is not consistent with a simple sequential pathway. However, whether these varying levels of protection indicate the existence of multiple rate-determining steps or rather the existence of multiple intermediate states is unclear, since it is quite likely that any structure in the β-domain that exists subsequent to the stabilization of the α-domain will be quite stable, i.e, have high protection factors. This is supported by the high stability of the α-domain intermediate to GdnHCl denaturation and the smaller guanidine dependence of the fast-phase rate constant, as shown in Figure 5, which suggest that the protein becomes much more compact after formation of the α-domain. The existence of multiple intermediates would explain time constants of amide protection that differ by an order of magnitude within the β-domain as well as significant levels of protection which occur in the β-domain prior to the attainment of tertiary structure as indicated by the near-UV CD.

The faster refolding of 3SS-lysozyme suggests that the non-native tertiary interactions observed during the refolding of unmodified lysozyme are *not* required for folding of this derivative. In the absence of the 6–127 disulfide bond, the α-domain is less stable and the formation of the non-native tertiary interactions is not observed. The folding pathways of 3SS-lysozyme and the unmodified protein are obviously different if one considers the sequence of intermediate states. The small fluorescence change observed during the refolding of 3SS-lysozyme suggests that the refolding of 3SS-lysozyme occurs in a concerted rather than in the stepwise fashion of the unmodified protein. The presence of the 6–127 disulfide bond clearly plays a role in directing the folding pathway of the unmodified protein.

However, the critical issue of whether the two proteins differ substantially in the structure of the final transition state of

folding is less clear. For example, it is possible that both 3SS-lysozyme and the unmodified protein refold through similar transition states and that the slower refolding of the unmodified protein arises as a result of the increased stability of the α-domain intermediate; viz., stabilization of an intermediate through interactions that do not stabilize the transition state which it precedes will result in an effective increase in the height of the activation barrier. Such an explanation is reasonable since it would seem unlikely that the non-native tertiary interactions which stabilize the α-domain would stabilize the final transition state of folding to the same extent. Alternatively, the transition state of folding could be very different for the two proteins, with the unmodified protein folding more slowly, possibly if the correct formation of the β-domain requires the disruption of the non-native tertiary interactions. Therefore, any questions regarding the similarities and differences of the transition state of folding for the two proteins will, in all likelihood, require mutational analysis to answer.

CONCLUSIONS

Based upon fluorescence- and absorbance-detected stopped-flow studies of unmodified and 3SS-lysozyme, interpreted in conjunction with existing literature, the major refolding pathway of unmodified lysozyme can be expressed by the following simple sequential model:

$$U \xrightarrow{\text{burst}} I_1 \xrightarrow{\text{very-fast}} I_2 \xrightarrow{\text{fast}} N$$

where U represents the unfolded protein, I_1 is the intermediate formed within the burst phase (the first 3 ms), I_2 is the intermediate formed during the very-fast phase, and N is the final native protein formed in the fast phase.

The first intermediate I_1 contains significant native structure in the α-domain, much of which is metastable. The α-domain becomes stabilized in the very-fast phase leading to the population of the second intermediate, I_2. I_2 is stabilized through the formation of non-native tertiary interactions which are manifested in the quenching of the fluorescence of a tryptophan residue, probably Trp-62 or Trp-108. The disulfide bond between Cys-6 and Cys-127 also plays an important role in stabilizing I_2, since the 3SS-lysozyme which lacks this disulfide bond refolds faster than the unmodified protein and without population of I_2. The final step (the fast phase) involves the correct folding of the β-domain which coincides with the formation of the native structure.

Added in Proof: After this paper was submitted, an article appeared (Itzhaki et al., 1994) describing a series of fluorescence-detected studies on lysozyme complementary to those presented here, which support many of the conclusions made here, most notably, that the final step in the folding of lysozyme involves disruption of nonnative interactions and that the folding pathways converge to a common rate-limiting step.

ACKNOWLEDGMENT

We thank S. Talluri, R. W. Ashton, and D. R. Buckler for helpful discussions, R. W. Dodge for assistance with the data processing, and W. A. Houry for improvements of the stopped-flow instrument and for critical reading of the manuscript. We also thank J. M. Beals and V. G. Davenport who, along with D.M.R., wrote the data acquisition program.

REFERENCES

Adler, A. J., Greenfield, N. J., & Fasman, G. D. (1973) *Methods Enzymol. 27*, 675–735.

Ahmad, F., & Bigelow, C. C. (1982) *J. Biol. Chem. 257*, 12935–12938.

Anfinsen, C. B. (1973) *Science 181*, 223–230.

Arnold, G. E., Day, L. A., & Dunker, A. K. (1992) *Biochemistry 31*, 7948–7956.

Aune, K. C., & Tanford, C. (1969) *Biochemistry 8*, 4579–4585.

Baldwin, R. L. (1993) *Curr. Opin. Struct. Biol. 3*, 84–91.

Blake, C. C. F., Koenig, D. F., Mair, G. A., North, A. C. T., Phillips, D. C., & Sarma, V. R. (1965) *Nature 206*, 757–761.

Chaffotte, A. F., Guillou,Y., & Goldberg, M. E. (1992) *Biochemistry 31*, 9694–9702.

Chan, H. S., & Dill, K. A. (1990) *Proc. Natl. Acad. Sci. U.S.A. 87*, 6388–6392.

Cooper, A., Eyles, S. J., Radford, S. E., & Dobson, C. M. (1992) *J. Mol. Biol. 225*, 939–943.

Creighton, T. E. (1986) *Methods Enzymol. 131*, 83–106.

Denton, M. E., & Scheraga, H. A. (1991) *J. Protein Chem. 10*, 213–232.

Dobson, C. M., Evans, P. A., & Radford, S. E. (1994) *Trends Biochem. Sci. 19*, 31–37.

Dodge, R. W., Laity, J. H., Rothwarf, D. M., Shimotakahara, S., & Scheraga, H. A. (1994) *J. Protein Chem.* (in press).

Dyson, H. J., & Wright, P. E. (1993) *Curr. Opin. Struct. Biol. 3*, 60–65.

Edelhoch, H., & Lippoldt, R. E. (1969) *J. Biol. Chem. 244*, 3876–3883.

Englander, S. W., & Mayne, L. (1992) *Annu. Rev. Biophys. Biomol. Struct. 21*, 243–265.

Formoso, C., & Forster, L. S. (1975) *J. Biol. Chem. 250*, 3738–3745.

Fukunaga, Y., Katsuragi, Y., Izumi, T., & Sakiyama, F. (1982) *J. Biochem. (Tokyo) 92*, 129–141.

Greene, R. F., Jr., & Pace, C. N. (1974) *J. Biol. Chem. 249*, 5388–5393.

Gregoret, L. M., & Cohen, F. E. (1991) *J. Mol. Biol. 219*, 109–122.

Hao, M.-H., Pincus, M. R., Rackovsky, S., & Scheraga, H. A. (1993) *Biochemistry 32*, 9614–9631.

Hao, M.-H., Rackovsky, S., Liwo, A., Pincus, M. R., & Scheraga, H. A. (1992) *Proc. Natl. Acad. Sci. U.S.A. 89*, 6614–6618.

Haynie, D. T., & Freire, E. (1993) *Proteins: Struct., Funct., Genet. 16*, 115–140.

Herning, T., Yutani, K., Taniyama, Y., & Kikuchi, M. (1991) *Biochemistry 30*, 9882–9891.

Hill, C. P., Johnston, N. L., & Cohen, R. E. (1993) *Proc. Natl. Acad. Sci. U.S.A. 90*, 4136–4140.

Houry, W. A., Rothwarf, D. M., & Scheraga, H. A. (1994) *Biochemistry 33*, 2516–2530.

Imoto, T., Johnson, L. N., North, A. C. T., Phillips, D. C., & Rupley, J. A. (1972a) in *The Enzymes (3rd Edition)* (Boyer, P. D., Ed.) Vol. 7, pp 665–868, Academic Press, New York.

Imoto, T., Forster, L. S., Rupley, J. A., & Tanaka, F. (1972b) *Proc. Natl. Acad. Sci. U.S.A. 69*, 1151–1155.

Inoue, M., Yamada, H., Yasukochi, T., Kuroki, R., Miki, T., Horiuchi, T., & Imoto, T. (1992) *Biochemistry 31*, 5545–5553.

Itzhaki, L. S., Evans, P. A., Dobson, C. M., & Radford, S. E. (1994) *Biochemistry 33*, 5212–5220.

Jennings, P. A., Saalau-Bethell, S. M., Finn, B. E., Chen, X., & Matthews, C. R. (1991) *Methods Enzymol. 202*, 113–126.

Kato, S., Okamura, M., Shimamoto, N., & Utiyama, H. (1981) *Biochemistry 20*, 1080–1085.

Kato, S., Shimamoto, N., & Utiyama, H. (1982) *Biochemistry 21*, 38–43.

Kim, P. S., & Baldwin, R. L. (1990) *Annu. Rev. Biochem. 59*, 631–660.

Kronman, M. J., & Holmes, L. G. (1971) *Photochem. Photobiol. 14*, 113–134.

Kumagai, I., Sunada, F., Takeda, S., & Miura, K. (1992) *J. Biol. Chem. 267*, 4608–4612.

Kuramitsu, S., Kurihara, S., Ikeda, K., & Hamaguchi, K. (1978) *J. Biochem. (Tokyo) 83*, 159–170.
Kuwajima, K. (1989) *Proteins: Struct., Funct., Genet. 6*, 87–103.
Kuwajima, K., Hiraoka, Y., Ikeguchi, M., & Sugai, S. (1985) *Biochemistry 24*, 874–881.
Kuwajima, K., Mitani, M., & Sugai, S. (1989) *J. Mol. Biol. 206*, 547–561.
Lehrer, S. S., & Fasman, G. D. (1967) *J. Biol. Chem. 242*, 4644–4651.
Longworth, J. W. (1966) *Biopolymers 4*, 1131–1148.
Matouschek, A., Kellis, J. T., Serrano, L., & Fersht, A. R. (1989) *Nature 340*, 122–126.
Matthews, C. R. (1993) *Annu. Rev Biochem. 62*, 653–683.
Miranker, A., Radford, S. E., Karplus, M., & Dobson, C. M. (1991) *Nature 349*, 633–636.
Montelione, G. T., & Scheraga, H. A. (1989) *Acc. Chem. Res. 22*, 70–76.
Oas, T. G., & Kim, P. S. (1988) *Nature 336*, 42–48.
Press, W. H., Flannery, B. P., Teukolsky, S. A., & Vetterling, W. T. (1990) *Numerical Recipes in C*, pp 542–547, Cambridge University Press, Cambridge, U.K.
Radford, S. E., Woolfson, D. N., Martin, S. R., Lowe, G., & Dobson, C. M. (1991) *Biochem. J. 273*, 211–217.
Radford, S. E., Dobson, C. M., & Evans, P. A. (1992) *Nature 358*, 302–307.
Rothwarf, D. M., & Scheraga, H. A. (1993a) *Biochemistry 32*, 2671–2679.
Rothwarf, D. M., & Scheraga, H. A. (1993b) *Biochemistry 32*, 2680–2689.
Schellman, J. A. (1978) *Biopolymers 17*, 1305–1322.
Scheraga, H. A., Konishi, Y., & Ooi, T. (1984) *Adv. Biophys. 18*, 21–41.
Shortle, D. (1992) *Q. Rev. Biophys. 25*, 205–250.
Smith, L. J., Sutcliffe, M. J., Redfield, C., & Dobson, C. M. (1993) *J. Mol. Biol. 229*, 930–944.
Strynadka, N. C. J., & James, M. N. G. (1991) *J. Mol. Biol. 220*, 401–424.
Tanaka, F., Forster, L. S., Pal, P. K., & Rupley, J. A. (1975) *J. Biol. Chem. 250*, 6977–6982.
Tanford, C. (1968) *Adv. Protein Chem. 23*, 121–282.
Teichberg, V. I., & Sharon, N. (1970) *FEBS Lett. 7*, 171–174.
Teichberg, V. I., Kay, C. M., & Sharon, N. (1970) *Eur. J. Biochem. 16*, 55–59.
Weissman, J. S., & Kim, P. S. (1991) *Science 253*, 1386–1393.
White, F. H., Jr. (1982) *Biochemistry 21*, 967–977.
Yamasaki, N., Eto, T., Abe, K., & Yamashita, S. (1990) *Agric. Biol. Chem. 54*, 1883–1884.